

Supporting Information

Xiaomin Li^a, *Jinwei Miao*^b, *Fulong Hu*^a, *Kang Yan*^b, *Lin Song*^a, *Huiqing Fan*^b,

Longtao Ma^c, *Weijia Wang*^{b,*}

Experimental section

Assembly of Zn||MnO₂ full cells

In order to prepare the cathode, MnO₂ active substance, Ketjen Black and polyvinylidene fluoride (PVDF) are mixed in the weight ratio of 7:2:1, and N-methyl-2-pyrrolidone (NMP) is used as the solvent, and ground into a fine slurry uniformly coated onto carbon cloth, which is dried at 60°C for 4h in the vacuum drying oven.

Characterization

In this experiment, the physical characterization of zinc foils, by-productions and SEI are mainly carried out by X-ray diffraction (XRD, Bruker, D8 Advance) and X-ray photoelectron spectroscopy (XPS, PHI 5000 Versa Probe III). The coordination state of Zn²⁺ in aqueous solution is detected by Raman spectroscopy (WITec, Alpha 300R) and Fourier Transform Infrared spectrometer (FTIR, Bruker, Tensor II). In order to confirm the surface morphology of the zinc foils after cycling, the surface are observed using Field Emission Scanning Electron Microscope (FESEM, SEISS, Gemini SEM 300), and SEI is observed by transmission electron microscopy (TEM, FEI, Talos F200X).

Calculation methods

The binding energies, electrostatic potential map, and HOMO-LUMO energy levels are conducted using the DMol3 program package in Materials Studio.^[33] The

exchange and correlation terms are determined using the generalized Gradient Approximation (GGA) in the form proposed by Perdew, Burke, and Ernzerhof (PBE). The energy convergence criterion is set to 10^{-5} Hartree.

The adsorption of FA, H₂O on the Zn (002) and (100) surfaces, and the adsorption between Zn²⁺, H₂O, and FA are investigated in this work. In surface adsorption model, there is about 15 Å vacuum for erasing the effect of periodic condition for slab model in the Z direction.

The binding energies are calculated with the following equation:

$$E_{\text{adsorb}} = E_{\text{A+B}} - E_{\text{A}} - E_{\text{B}}$$

E_{adsorb} is energy of adsorption. $E_{\text{A+B}}$, E_{A} and E_{B} are the total energies of the system, A and B, respectively. A, B represent interfaces, Zn²⁺, FA or H₂O.

MD simulations are performed by the Forcite module in Materials studio to explore the solvation structure of Zn²⁺. The COMPASSII force field are selected for assigning charges of Zn²⁺, SO₄²⁻ and FA. First, the geometry optimization is carried out in the Forcite module, in which the lattice geometry is optimized based on the convergence of the total energy (0.0001 kcal mol⁻¹) with the force of 0.005 kcal mol⁻¹Å⁻¹. After that, the MD simulations are conducted by NVT and NPT ensembles at 298K. The cutoff distance for van der Waals and the electrostatic interactions are both 15.5Å. All simulations are carried out in the standard periodic boundary condition and the simulation time is long enough to ensure being the equilibrium states of the electrolyte systems.

Electrochemical Tests

The manufactured CR2032 coin cells are subjected to galvanostatic charge-discharge (GCD) tests using two battery test systems, LANHE CT3002A and NWEARE CT-4008, with different charge/discharge regimes for different batteries, as shown below:

Zn||Zn symmetric battery:

Charge to a certain capacity at a constant current, then discharge to this capacity at the same constant current, recorded as one charge/discharge cycle, at the same time the changes of voltage with time are recorded.

Zn||Cu asymmetric battery:

After discharging with a certain current at a constant current for 2h, then charging with the same current to 0.5V, and then discharging with this current to a cut-off capacity of 0.5mAh as one charging/discharging cycle. The Coulombic efficiency of this charge/discharge cycle is the ratio of the charging power to the discharging power, and then the change of the Coulombic efficiency with cycle number and the voltage change in the charge/discharge process are recorded.

Zn||MnO₂ full cell:

The charging and discharging voltage range is 0.8-1.85V, and the long cycle performance is tested at a current density of 1 A g⁻¹, and the rate performance is tested at the current density of 0.5-10 A g⁻¹, respectively.

Linear Scanning Voltammetry (LSV), Tafel, Chronoamperometry (CA), Cyclic Voltammetry (CV), and Impedance Spectroscopy (EIS) are all performed through an electrochemical workstation (CORRTEST CS2350M). LSV is a steady-state test

method, also known as the controlled potential method, that discusses the relationship between current and voltage. The hydrogen evolution overpotential of Zn||Cu is investigated using this method with a scanning range of -0.3 to 0.15 V and a scanning rate of 1.0 mV s⁻¹. Tafel curve test is also a steady state test method to discuss the relationship between current and voltage. Tafel curves of Zn||Zn symmetric batteries with various electrolyte systems are tested using electrochemical workstation. The voltage interval is -0.25 to -0.25 V and the scanning rate is 1 mV s⁻¹. The potential step method, also known as chronoamperometry (CA) is a transient test method that discusses the relationship between current and time. The initial voltage polarization enables the ion diffusion behavior at the electrode surface to be probed. The current-time curves of Zn||Zn symmetric batteries are tested using a step voltage of -200 mV for 300 s. Cyclic voltammetry (CV) refers to the transient study method with constant scan rate to discuss the relationship between current and voltage. A two-electrode system is used, with a voltage interval of -0.3 to 0.9 V and a sweep rate of 1 mV s⁻¹ for Zn||Cu cells, and a voltage interval of -0.8 to 1.85 V and a sweep rate of 1 mV s⁻¹ for Zn||MnO₂ batteries. The EIS is also a transient measurement method to directly measure the AC impedance of a system using a small amplitude sinusoidal AC signal as a perturbation signal. Zn||MnO₂ full cells and Zn||Zn symmetric batteries are tested using a two-electrode system with an amplitude of ± 5 mV and a frequency range of 10 mHz to 100 kHz.

The Ionic conductivity of the electrolytes is measured through EIS with cells consisted of two parallel Ti-plate electrodes (1 cm²). The electrode resistance is

obtained from the intercept of Nyquist plot and the ionic conductivity is calculated according to the following equation:

$$\sigma = \frac{L}{RS}$$

where σ is the per unit conductivity, R is the diffusion resistance, L is the interval distance between the two Ti-plate electrodes, S is electrode area.

The electrochemical impedance spectroscopy (EIS) for evaluating Zn^{2+} transference number is collected within 10^{-2} ~ 10^{-5} Hz at an AC voltage of 10 mV in a symmetric Zn||Zn testing system. The chronamperometry measurement is implemented by imposing a bias voltage of 10mV for 2000 s, followed by another AC impedance measurement. The Zn^{2+} transference number (t) is calculated by the following equation:

$$t = \frac{I_s(\Delta V - I_1 R_I)}{I_1(\Delta V - I_s R_s)}$$

Where ΔV is the bias voltage, R_I and R_s are the initial and steady-state charge transfer resistances of the electrode, and I_I and I_s are the initial and steady-state current, respectively.



Fig. S1 Photographs of electrolytes with different FA ratios after standing for one month.

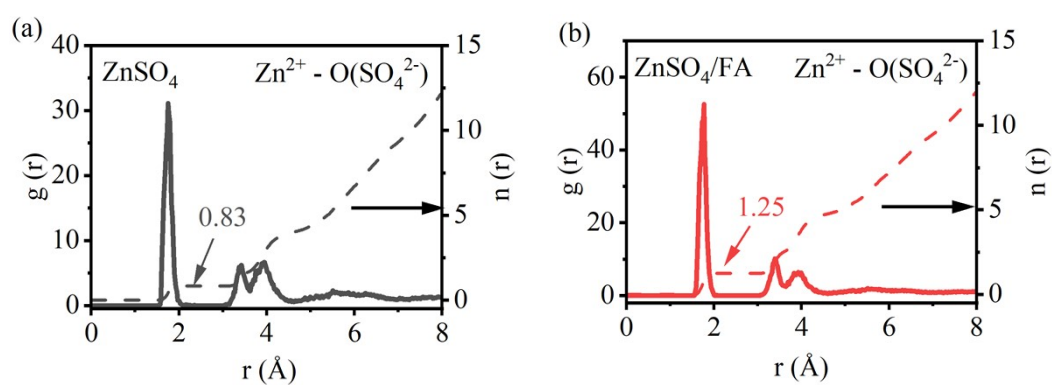


Fig. S2 Radial distribution function (RDF) of $\text{Zn}^{2+}-\text{O}(\text{SO}_4^{2-})$ in (a) pure ZnSO_4 electrolyte and (b) ZnSO_4/FA electrolyte.

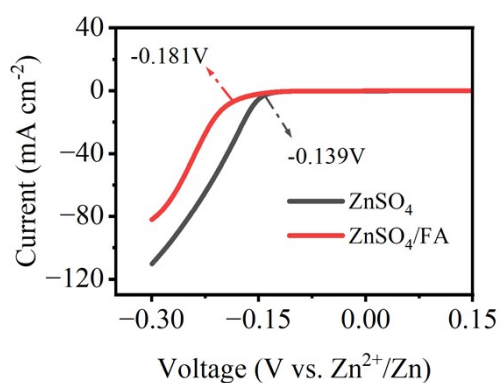


Fig. S3 Hydrogen evolution reaction (HER) performance of the Zn anode in the pure ZnSO_4 electrolyte and ZnSO_4/FA electrolyte.

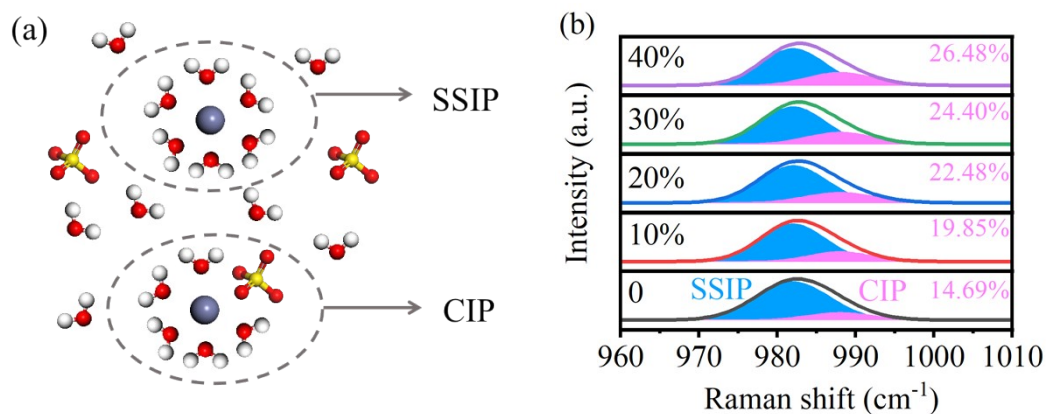


Fig. S4 (a) Schematic illustration of solvent separated ion pair (SSIP) and contact ion pair (CIP). (b) Raman spectra for ZnSO₄ electrolytes without and with various concentrations of FA.

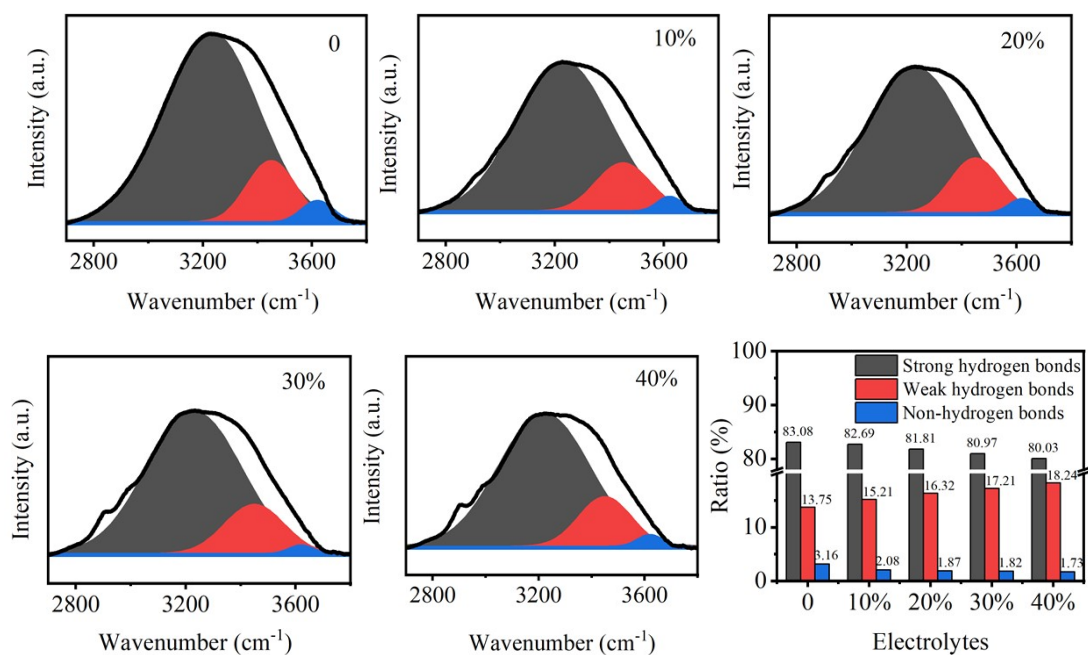


Fig. S5 Strong hydrogen bonding, weak hydrogen bonding and non-hydrogen bonding in ZnSO₄ electrolytes without and with various concentrations of FA.

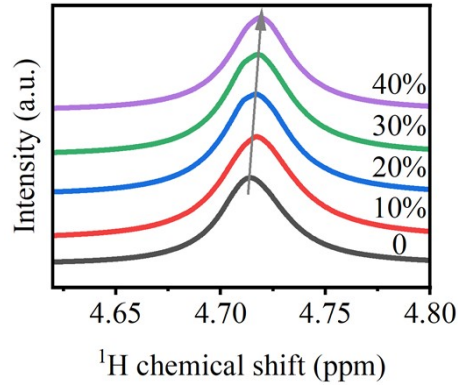
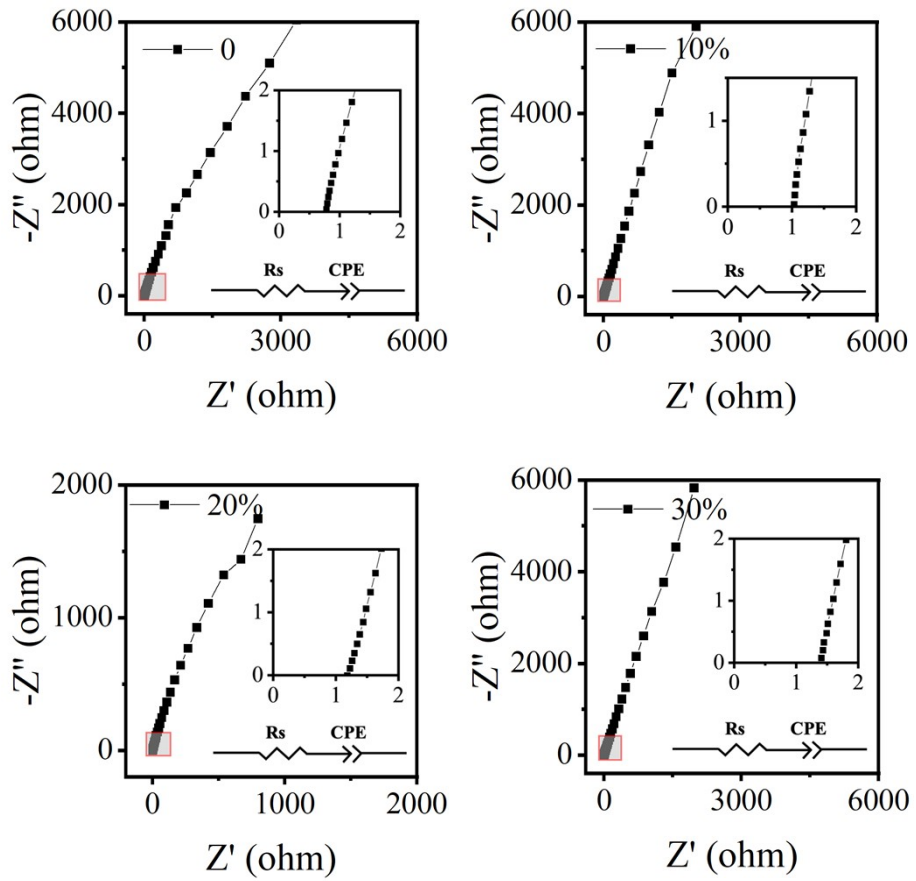


Fig. S6 NMR spectra of ZnSO₄ electrolytes without and with various concentrations of FA.



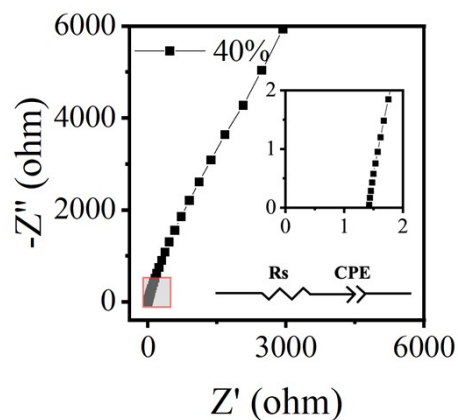


Fig. S7 Test details for ionic conductivity in $ZnSO_4$ electrolytes without and with various concentrations of FA.

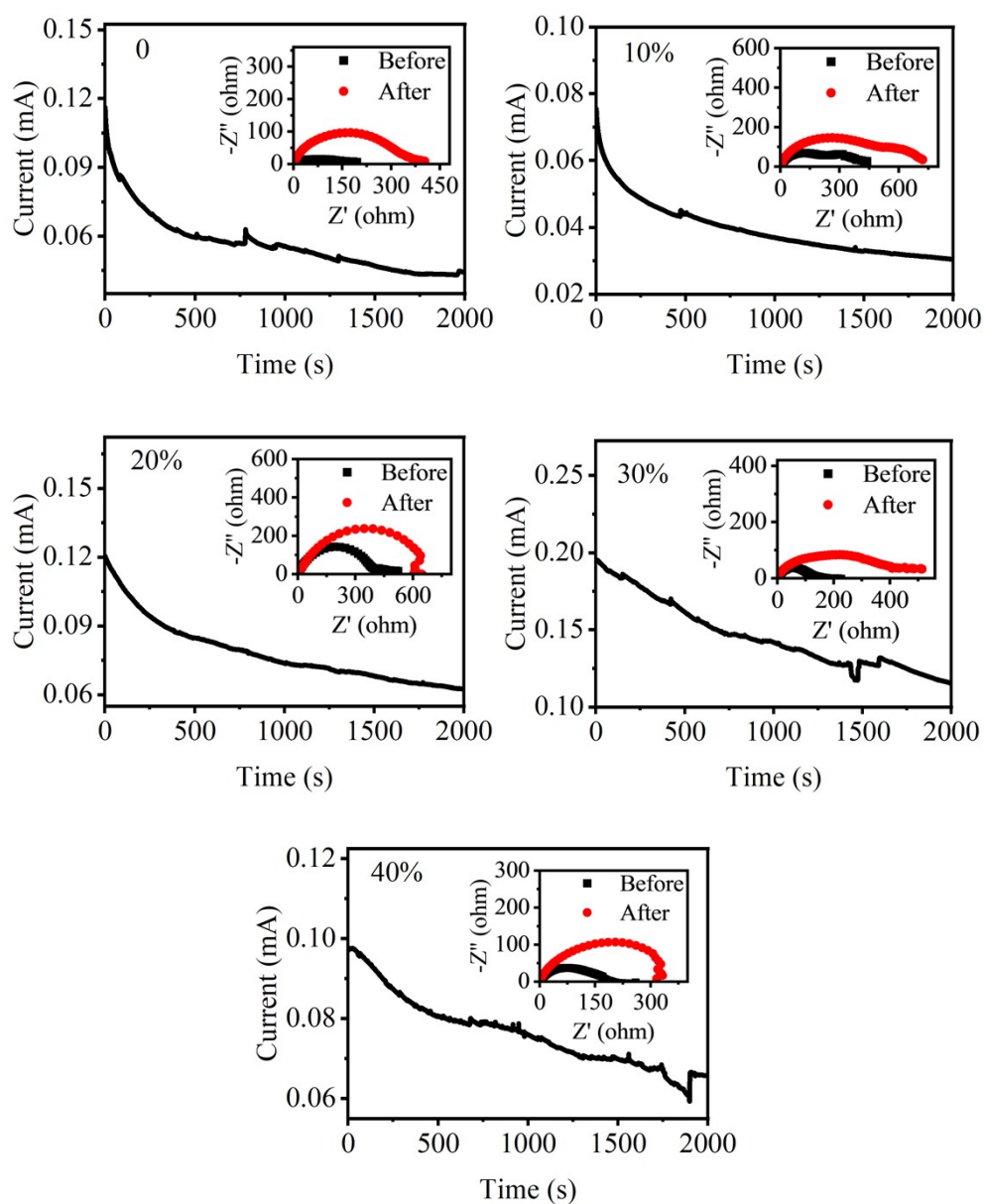


Fig. S8 Test details for transference number of Zn^{2+} in ZnSO_4 electrolytes without and with various concentrations of FA.

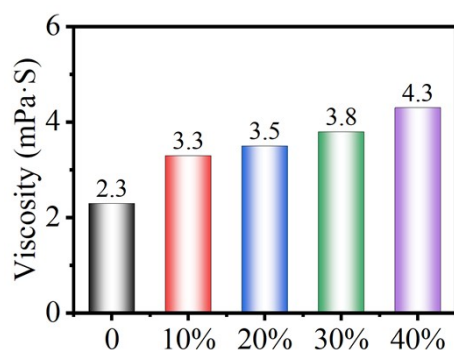


Fig. S9 Viscosity of ZnSO_4 electrolytes without and with various concentrations of FA.

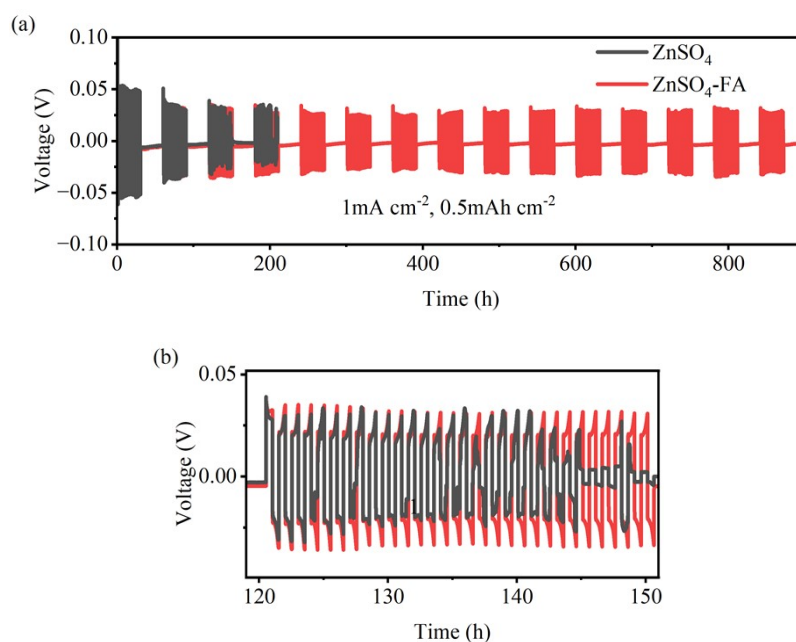


Fig. S10 (a) Dynamic measurement of $\text{Zn}||\text{Zn}$ symmetric batteries at current density of 1 mA cm^{-2} with capacity of 0.5 mAh cm^{-2} by resting 30h after cycling 30h and (b) the partial enlarged detail.

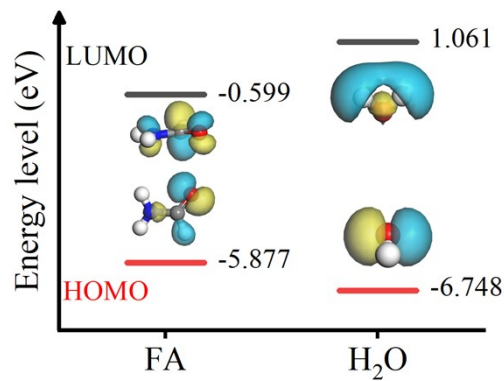


Fig. S11 LUMO and HOMO orbital energy levels of FA and H₂O molecules.

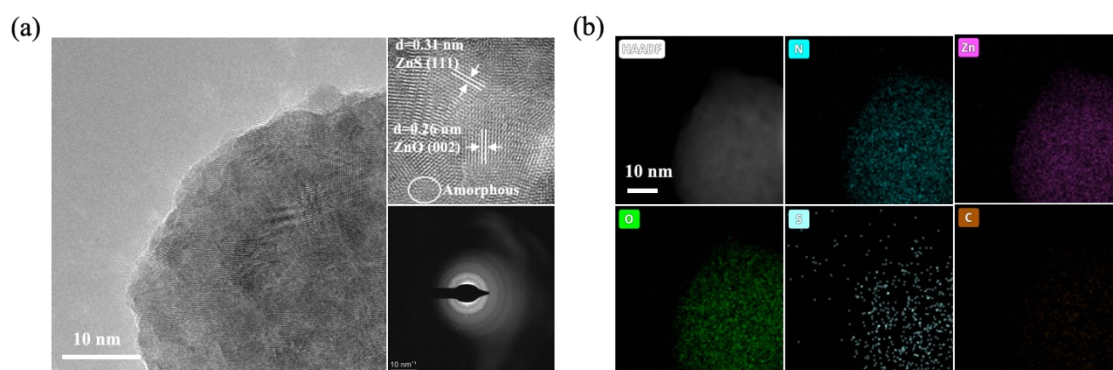


Fig. S12 (a) TEM, HR-TEM images and SAED of SEI formed in the ZnSO₄/FA electrolyte. (b) HAADF image and corresponding elemental mapping of the sample.

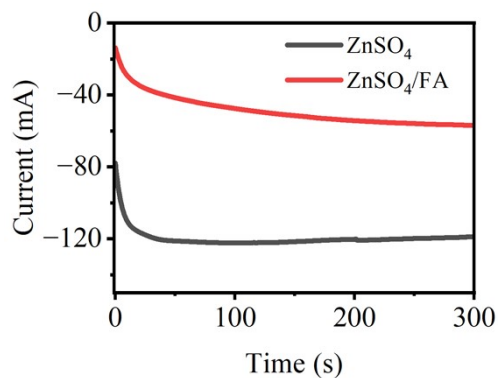


Fig. S13 CA curves of pure ZnSO₄ electrolyte and ZnSO₄/FA electrolyte under a voltage of -200 mV.

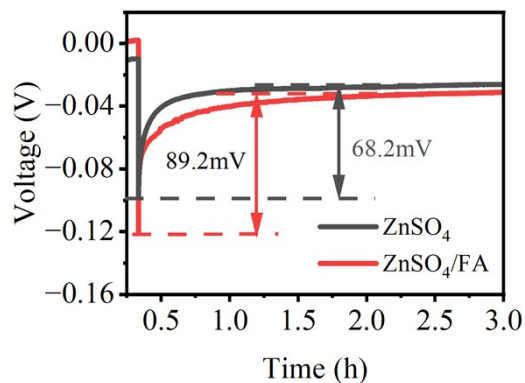


Fig. S14 Nucleation and growth overpotentials of Zinc in pure ZnSO_4 electrolyte and ZnSO_4/FA electrolyte.

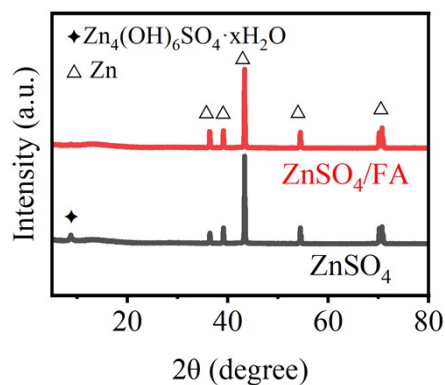


Fig. S15 XRD patterns of Zn anode after 20 plating/stripping cycles in pure ZnSO_4 and ZnSO_4/FA electrolyte under current density of 1 mA cm^{-2} with a capacity of 0.5 mAh cm^{-2} .

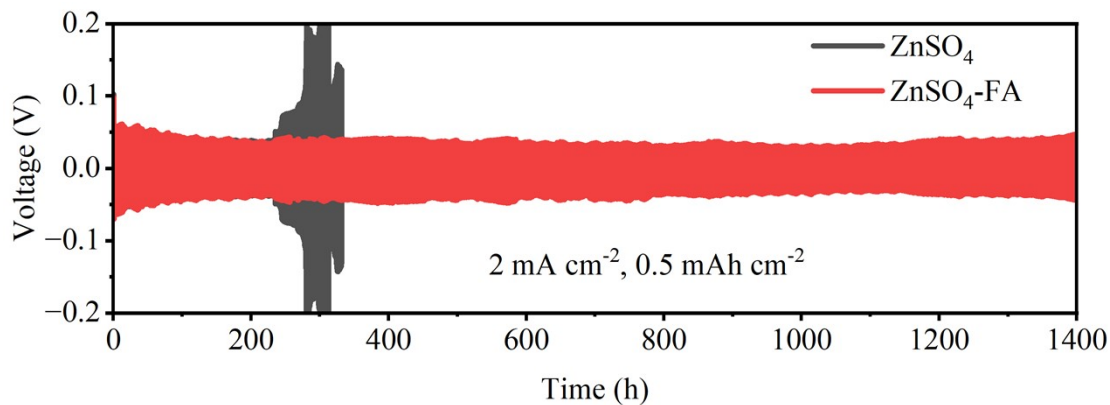


Fig. S16 Cycling performance of Zn/Zn symmetric batteries at 2 mA cm^{-2} , 0.5 mAh cm^{-2} .

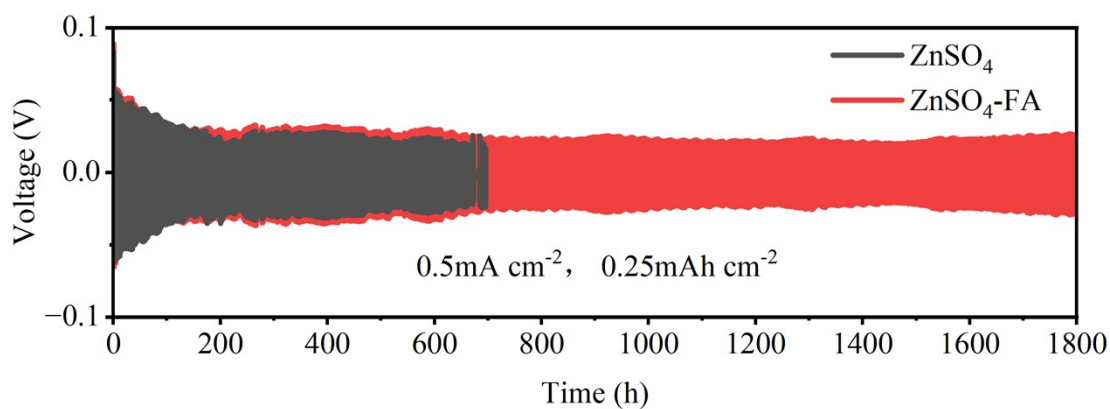


Fig. S17 Cycling performance of Zn||Zn symmetric batteries at 2 mA cm⁻², 0.5 mAh cm⁻².

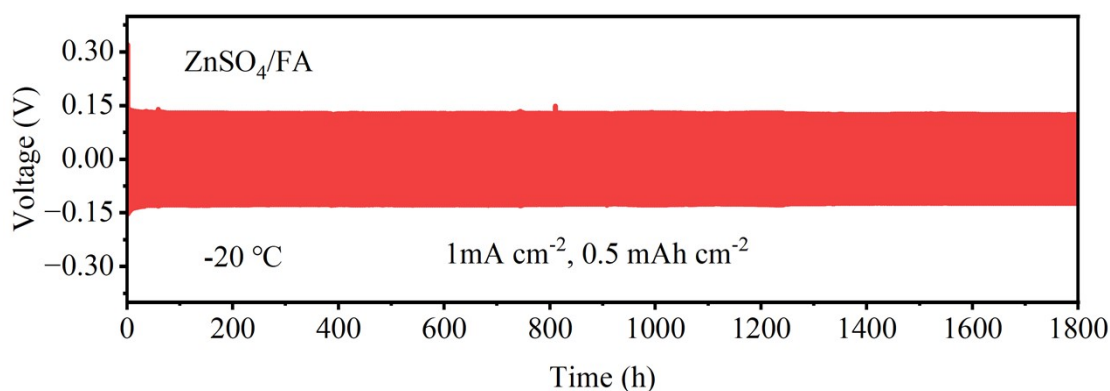


Fig. S18 Cycling performance of Zn||Zn symmetric batteries at 1 mA cm⁻², 0.5 mAh cm⁻² at -20°C.

Table S1. Voltage hysteresis of Zn||Zn symmetric batteries at different current densities.

Electrolyte	0.5	1	2	5	8	10	15
ZnSO ₄	108.4	109.4	103.2	98.7	100.3	105.1	141.6
ZnSO ₄ /FA	100.8	98.8	101.9	150.7	157.5	144.3	